World Scientific
www.worldscientific.com

Intense ionizing radiation from laser-induced processes in ultra-dense deuterium D(−1)

Frans Olofson and Leif Holmlid*

Atmospheric Science,
Department of Chemistry and Molecular Biology,
University of Gothenburg,
SE-412 96 Göteborg, Sweden
*holmlid@chem.gu.se

Nuclear fusion in ultra-dense deuterium D(−1) has been reported from our laboratory in a few studies using pulsed lasers with energy < 0.2 J. The direct observation of massive particles with energy 1–20 MeV u^{-1} is conclusive proof for fusion processes, either as a cause or as a result. Continuing the step-wise approach necessary for untangling a complex problem, the high-energy photons from the laser-induced plasma are now studied. The focus is here on the photoelectrons formed. The photons penetrating a copper foil have energy > 80 keV. The total charge created is up to 2 μC or 1×10^{13} photoelectrons per laser shot at 0.13 J pulse energy, assuming isotropic photon emission. The variation of the photoelectron current with laser intensity is faster than linear for some systems, which indicates rapid approach to volume ignition. On a permanent magnet at approximately 1 T, a laser pulse-energy threshold exists for the laser-induced processes probably due to the floating of most clusters of D(−1) in the magnetic field. This Meissner effect was reported previously.

1. Introduction

The ultra-dense material D(−1) named ultra-dense deuterium is superfluid at room temperature. Its behavior in production and transport for use as a fuel for inertial confinement fusion (ICF) is thus not easily understood. Further, its behavior during the energy generating laser-induced fusion processes[1–5] also needs to be better characterized. It has a normal bond distance of 2.3 pm which may even give a small rate of spontaneous fusion. The density of this material is close to 10^{29} cm^{-3} or 140 kg cm^{-3}.[6–18] The extremely high density of D(−1) means that the Lawson

criterion $n\tau \geq 10^{22}$ m^{-3} s for D+D fusion only requires a confinement time τ of 0.2 ps. The temperature of > 100 MK required for fusion is indeed observed.[2] It seems that laser pulses of < 1 J pulse-energy are enough to reach break-even.[4,5] This low energy requirement is of course due to the high density of D(-1), which means that this material may be the fuel of choice for laser-initiated ICF (inertial confinement fusion).[19,20] The fusion process has so far mainly been investigated with nanosecond pulsed lasers, but a study with a picosecond-pulsed laser was recently completed.[21]

Several methods have been studied to reach ignition of nuclear fusion in a controlled way, but none has yet been able to reach break-even for any prolonged period of time. Both magnetically and inertially confined methods are under active development. The largest laser-initiated ICF research laboratory developed so far is undoubtedly the National Ignition Facility (NIF) in USA.[22] It uses a mixture of T and D as fusion fuel. This is considered to be a factor of 30 easier to ignite than the pure D fuel studied in the present work. However, this fusion fuel is at the start at normal hydrogen ice density, and it needs to be compressed by a large number of laser beams. In a recent report so called scientific break-even was reported from NIF.[23] The large problems with reaching this stage can probably be attributed to the formation of ultra-dense hydrogen H(-1) during the laser-compression in NIF giving strong instabilities.[24] Thus, it is likely that laser-compression of a low-density fuel used is not the best process to be used for future fusion energy production. One of the drawbacks of using the T+D fuel for energy production is also the necessary production and handling of T (this drawback may also exist for magnetically confined fusion). Tritium is easily inhaled (especially in its oxidized form as water) and has low-energy beta radioactivity which makes it difficult to monitor. Another problem with the D+T system is the high neutronicity of 0.80, which means that 80% of the energy from the fusion process is given to neutrons and thus difficult to use for efficient power production. Only 20% is given to charged particles. If a relatively high conversion efficiency to electric power of 40% is assumed for example in an ordinary steam cycle, only 8% of the total fusion energy will be converted to useful work. In general, D as fusion fuel (as used here) gives considerably lower neutronicity, and 34–62% of the energy is found in charged particles. Thus, if large-scale fusion in pure D can be developed, the problems with T handling and with the low energy conversion efficiency of the D+T process would be circumvented. The main benefit of using ultra-dense deuterium as fusion fuel (as here) is that the fuel density at the start is very high and no compression lasers are needed, thus also giving a much higher energy gain relative to the laser input power. Only an igniting laser is required, in some aspects similar to the proposed "fast" ignition ICF method.[25,26] We have shown in several publications that fusion in ultra-dense deuterium is observed for example by the ejection of large fluxes of massive particles with energy of 1–20 MeV u^{-1}.[4,5,27] Measuring the particle flux absolutely as a function of time provides the possibility to calculate the energy given to these particles, which is found to be several J per laser shot, even with laser pulses of only

0.1 J. Thus, a large energy gain is found.[5] So far, the main disadvantage observed with this approach is the difficulty to handle the superfluid fuel. This means that the total output energy is still relatively low due to the small amount of material that can be easily assembled and fused around the laser focus.

The velocity distributions for the particles with 1–20 MeV u^{-1} from the laser fusion are almost thermal.[27] This indicates the occurrence of fusion in the laser-induced processes, either as a source or as a result of the multi-MeV particles. With this background, we now investigate the processes involved in the production and detection of ionizing photons, mainly contributing to photoelectrons from surfaces in the apparatus. The number of such photons is a measure of the energy released in the fusion process, and the variation with laser pulse energy of the total charge created is investigated. A faster than linear variation is of course required for ignition, and such a variation is observed for special systems. This investigation is part of a program to understand the fusion processes in the ultra-dense deuterium D(−1) fuel. This is done by defining and developing suitable experiments to prove different partial processes and particles ejected in the processes. We also use standard methods for characterization and identification of particles and processes. Due to the complexity of the processes and particles observed, a battery of methods is not a useful approach as known from many scientific fields. Conversely, the stepwise approach has proved its value in our studies, for example in the detection and investigation of the unexpected neutral particles with energy of 1–20 MeV u^{-1}.[3–5,27] Further studies of such particles are submitted.

2. Theory

The inter-atomic distance in the common form of ultra-dense deuterium D(−1) is approximately 2.3 pm.[6–18] The most exact measurement done on the clusters of the form D$_4$ gives 2.15 ± 0.02 pm.[15] Other excitation levels with other bond distances exist. The material D(−1) is a quantum material.[28] It may contain vortices in a Cooper pair electron fluid.[29,30]. The molecular structure of D(−1) is given by chain clusters D$_{2N}$ with N integer, formed by D–D pairs rotating around the vortex.[14,17] D(−1) is superfluid[28] at room temperature and forms thin layers on various surfaces, mainly on metal surfaces.[4,31] Thus, it cannot be retained in a container with any kind of opening and will not stay where it is deposited. In experiments, it is shown to creep on to the back side of foils[14] and creep up and down on vertical surfaces easily.[18] A so called fountain effect is also observed,[14] which requires a long-lived moving film on the surface studied. Since it is superfluid, it may easily absorb photons and transport the absorbed energy within the material. On polymer surfaces, a superfluid film is not formed.[31] A Meissner effect is observed for D(−1) at room temperature,[32] which indicates that D(−1) is superconductive. The Meissner effect means that the clusters of D(−1) float in a magnetic field above the magnet. The experiments show that small clusters like D$_4$ still exist on the magnet surface, probably since they are symmetric and do not have a magnetic dipole moment.

There is no indication in any experiments that D(−1) is short-lived. Quite oppo-site, D(−1) is stable for days and weeks even in a vacuum[12] and can be detected by the first laser pulse in the experiments. It is observed that thicker layers of D(−1) exist at edges and at wires on surfaces, which means that D(−1) is a liquid with surface tension. During an experimental run of a few hours, the amount of D(−1) increases on the target surface. Such effects would not exist with life-times of D(−1) less than several hours.

The initiation of nuclear fusion in D(−1) is a complex process with several important features. First, it is very clear that the D–D distance of 2.3 pm normally observed is so short that some tunneling giving D+D fusion may take place even without laser induction.[29,30] The 2.3 pm distance corresponds to an excitation level $s = 2$ for the spin-based structure in D(−1). In the lowest spin level $s = 1$, the D–D distance is only 0.56 pm[33] as observed experimentally. This short D–D distance implies that it is not necessary that fast particles are formed in D(−1) to initiate fusion, but it is probably enough that the system is de-excited to the lowest level $s = 1$ for the fusion process to take place spontaneously. It is possible, though, that this lowest quantum level $s = 1$ is at a higher energy level than $s = 2$, and that the laser pulse induces the transfer to this lowest quantum level from where the fusion process takes place rapidly.

It is further known that energetic particles (deuterons) are released in the D(−1) material by several processes. The laser induces Coulomb explosion processes which give a kinetic energy release (KER) of 630 eV in each ion-pair explosion in D(−1) at $s = 2$.[6,10] Similar three-charge processes at $s = 2$ give a KER of 1260 eV.[11] The level $s = 1$ gives a KER of 2580 eV,[33] which will give fusion. A process named laser-initiated self-compression is also proposed to be responsible for ejection of MeV particles in D(−1). This type of process was studied in ultra-dense protium p(−1)[34] where normal fusion processes should not be possible. It is assumed to take place also in D(−1) but is difficult to study in that system directly due to the fusion processes taking place. The laser-induced processes generate a high temperature in the plasma, above 100 MK.[2]

3. Experimental Method

The experimental setup is shown in Fig. 1. The laser used is a Nd:YAG laser with pulse energy < 0.2 J at 532 nm used in most experiments. In a few cases, 1064 nm light at energy < 0.4 J is used. The pulses are 5 ns long. The repetition rate is varied between 2 and 20 Hz with 10 Hz as standard. The laser is focused on a metallic target plate with a 50 mm focal length lens. This lens can be moved in half a circle around the center of the horizontal target plate, while the target plate can also be turned around this center. The laser beam waist is < 20 μm calculated for a Gaussian beam. D(−1) is produced in a source containing catalyst samples (potassium doped iron oxide catalysts, so called styrene catalysts[35,36]) from deuterium gas (99.8%) at a pressure up to a few millibar. The lower end of this source is located a few mm
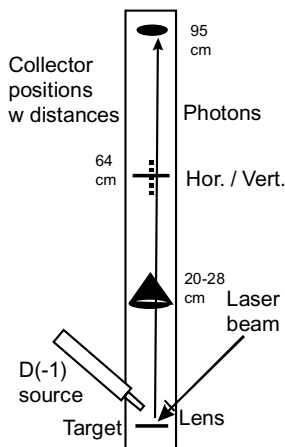
Fig. 1.   Principle of the apparatus used, vertical cut, with three simultaneous collectors. Collectors are used at other distances as well as given in the figure captions. A similar source is described in Ref. 13.

above the target plate. In the stainless steel target plates, vertical holes are bored which hold samples of Ir metal. In the magnet experiments, a NdFeB magnet (SSG N33SH) with dimensions $3 \times 4 \times 8$ mm^3 gives a magnetic field strength up to 0.17 T at 1.0 mm distance on the target, with one of the largest faces (the pole faces) exposed to the laser. The manufacturer states that the remanent field strength B_r is > 1.1 T.

The main signal studied here is due to photoemission of electrons from the collectors. Several different collectors have been used. An Al collector with 3 mm thickness and a diameter of 80 mm is mounted above the target at a distance of 44 cm (not included in Fig. 1). An inverted cone-shaped collector of 0.5 mm thick Cu plate is used at a variable 20–28 cm distance. The cone form means that the distance for penetration through the material is 1 mm. Another collector which can be rotated into the vertical or horizontal positions (as shown in Fig. 1) is 1.5 mm thick Al at a distance of 64 cm. The current to the collectors is taken out via a short 50 Ω coaxial cable to the 50 Ω input of a fast digital two-channel oscilloscope (Tektronix TDS 3032, 300 MHz). Thus, a signal of 1 V corresponds to 20 mA of current. Battery bias of the collectors is used in the present study only for characterizing the signals. Thus, zero bias is normally used in the experiments.

The signal from the collector in the oscilloscope has a resolution of 0.2 ns. By summing the current in the time distribution observed, the charge ejected at the collector and the number of photoelectrons is determined. It is assumed that the ejection of the photons at the target is isotropic, which means that the total charge is calculated from the viewing angle of the collector used relative to the laser focus.

4. Results

An experiment with two collectors in-line is shown in Fig. 2. In the upper panel, the
time-base for the upper collector (at 95 cm distance) is shifted 1 ns to compensate
for the time for photons to move from the middle collector (at 64 cm) to the upper
one. The agreement between the two curves is good, indicating that photons are
almost the only type of particle detected under these conditions. In the lower panel,
the time-scale for the upper collector signal is recalculated by the factor 64/95,
to compensate for the difference in distances travelled by massive particles. No
agreement between the curves is found in this case. This shows that the signal is
due to photons and that the shape of the distribution, reaching above 100 ns, is
not due to a time-of-flight process for massive particles like ions, but is an intrinsic
time-dependence for the process of photon emission at the target.

The possibility that the second peak at 70 ns in Fig. 2 contains some signal
due to electrons from the target was tested, even if the sign of the signal does not
agree with an electron current. A TOF of 70 ns with a collector distance of 95 cm
means an energy of 500 eV for electrons moving from the target to the collector.
Such electrons will have a radius of their motion in the geomagnetic field of 1.5 m,
giving a deflection at 0.95 m of 0.3 m. They will thus reach the walls in the chamber
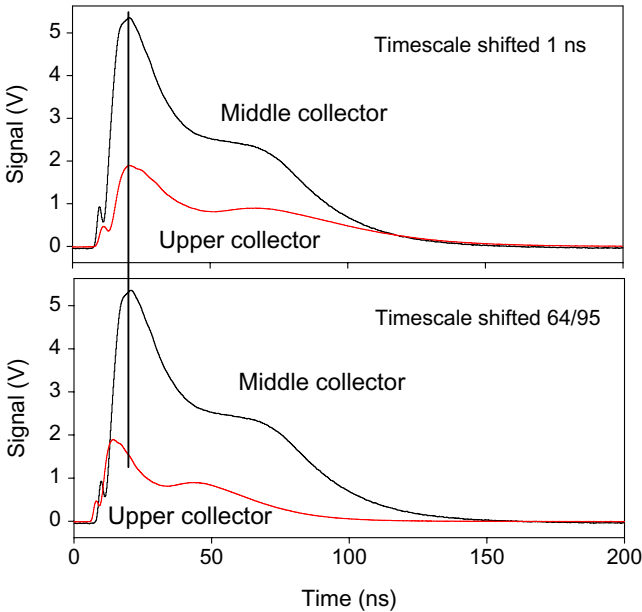

Fig. 2.   Signals from two collectors in-line at distances 64 and 95 cm. Zero bias. The lower collector
was rotated to vertical position when the upper collector signal was measured. The upper panel
shows the time-base shifted 1 ns for the upper collector due to velocity of light. The lower panel
shows the time-base shifted by factor 64/95 which is the scaling expected for massive particles.
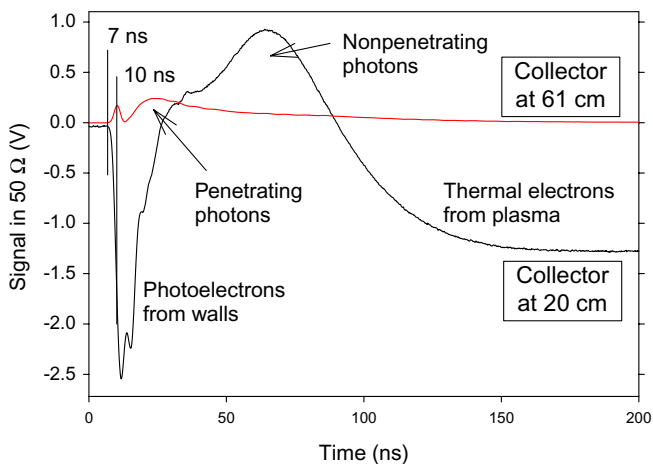532 nm, 125 mJ pulse-energy at 10 Hz.

Fig. 3.   Two collectors at 20 cm and 61 cm simultaneously, zero bias. Lower collector is fixed and photons are transmitted through 1 mm Cu to the second collector. 532 nm, 125 mJ pulse-energy at 10 Hz.

before reaching the collector. They will further not be able to easily pass the lower collectors.

It is possible to observe differences in the properties of different parts of this intrinsic photon time distribution. One example is given in Fig. 3. The signals with zero bias to two collectors in-line is shown there. The collectors are fixed and the one at 20 cm distance covers almost the whole internal apparatus opening. It is shaped as a cone with its opening toward the target, preventing scattering of photons and particles like ions and electrons around the edge. (Such scattering processes may be possible in the case of a flat collector.) Thus, the signal to the collector at 61 cm is due to penetrating photons or particles. The signal shape to this upper collector is similar to that observed generally for ionizing photons here, for example in Fig. 2. On the other hand, the bump in Fig. 3 at the first collector at 70 ns is due to photons that do not penetrate easily but ionize and are stopped by the first collector since they are not observed at the collector at 61 cm distance. This bump is at the same time as observed in Fig. 2 even at the upper collector, thus due to photons. From such results, it is concluded that the photon distribution from the target contains penetrating photons at times shorter than 30 ns, while at longer times, photons with lower energy are emitted from the target. The lower limit in photon energy that can penetrate 1 mm of copper in the cone collector is 80 keV. Thus, the first bump in Fig. 3 consists of photons with $E > 80$ keV, while the second bump has energy < 80 keV. Photons with low energy (visible) of course also exist, but they do not eject electrons from the metal surfaces in the apparatus since the work function for most metals is 4 eV, much larger the energy of the photons from the laser at 2.3 or 1.2 eV. The inverted copper cone collector is only used in Fig. 3 and not in the

other experiments. Otherwise, the electrons from the plasma in the other figures would not be observed.

Here we concentrate on the variation of this ionizing photon signal with laser intensity and laser pulse-frequency. One of the further parameters investigated is a constant magnetic field in the plasma region. Other parameters like the material sampled on the target and the wavelength of the laser are important but not investigated in detail here. However, such effects will be discussed below.

The signal varies in shape with the distance from the target. In Fig. 4, the collector is at 44 cm distance and the laser pulse-frequency is varied. The variation of the signal with distance is partially due to the larger projected wall area close to the collector which is exposed to the ionizing photons with a collector at short distance. This effect is seen in Fig. 4, where an intense first negative spike is due to fast electrons from the surrounding walls, possibly mainly due to Compton scattering. However, photoelectrons may also have a high energy, depending on the ionizing photon energy. This first intense negative peak is normally not observed with collectors at longer distance, but may be replaced with a positive peak instead which is probably due to Compton electrons or photoelectrons ejected from the collector. The distributions of photons in Fig. 4 can be understood as a first period
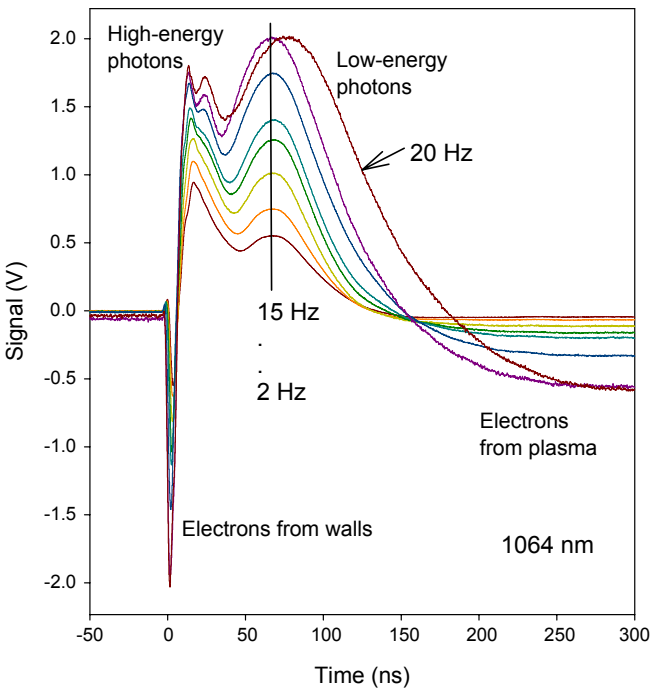

Fig. 4. Variation of the collector signal at 44 cm distance with laser pulse-frequency. Ir surface sampled, 0.1 mbar D_2 pressure, 1064 nm light. Laser pulse-energy at 10 Hz approximately 300 mJ. Zero bias.

with ejection of high-energy photons from the high-temperature process, and a later period with photon production from the cooling plasma. Another feature in Fig. 4 is the increasing negative signal at long times, caused by electrons from the plasma at the target. This signal is not observed at longer distances, since these low energy electrons will be deflected by the geomagnetic field and reach the chamber walls before reaching a distant collector.

In Fig. 5, the general picture with variation of the laser pulse-energy in these experiments is shown. In panel (a), the signal shows a negative first spike, and two peaked areas of low and high energy photons. Also, a slower electron current from the plasma is apparent. The positive charge for each curve is plotted in panel (b) as
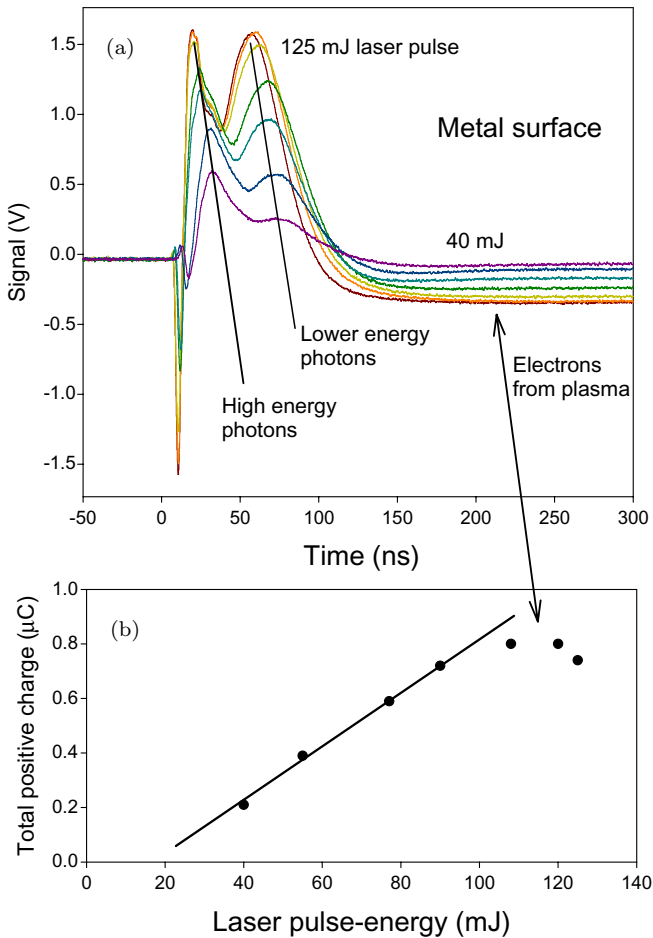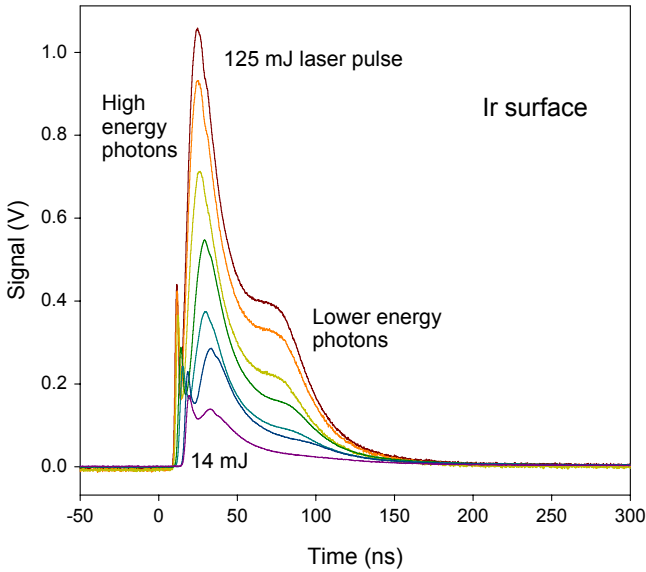

Fig. 5.   Variation of the collector signal at 44 cm distance with laser pulse-energy in panel (a). The target was stainless steel, laser 532 nm. The collector covered a fraction 2.1×10^{-3} of the full sphere. The positive charge in each curve is converted to the total charge per laser pulse assuming isotropic light emission in panel (b).

a function of the laser pulse-energy. The number of charges observed at the collector is divided by the fraction of the full sphere covered by the collector used around the laser focus. Thus, the total positive charge observed due to photoemission is plotted in panel (b), assuming isotropic photon emission from the target. The charge formed by the photons increases linearly with pulse-energy up to a point where it levels off and starts to decrease. This may be due to a limiting in the laser-induced process, but in the present case it is probably related to the intense electron current from the plasma observed in the upper panel in Fig. 5. This current decreases the apparent signal. The total positive charge formed is up to 1 μC or 6×10^{12} charges per laser shot by impact of the ionizing photons on the metal parts of the apparatus.

Using other materials as the target gives other features. In Fig. 6, the behavior with an Ir cylindrical piece as the target is shown when the laser pulse-energy is varied. The collector is at 95 cm distance, which means that the first negative spike is replaced by a positive one, probably due to Compton scattering at the collector. The peak with high-energy photons is relatively much larger in this case with an Ir target. Further, the total charge formed is plotted in panel (b) and shows a linear variation with pulse-energy at low energy, but a faster variation with pulse-energy at the highest pulse-energies. This effect is of course very interesting for attempts to reach volume ignition. The total charge is also larger than in Fig. 5, up to 2.2 μC or 1.4×10^{13} charges per laser shot.

It was shown in other types of experiments that ultra-dense deuterium probably is superconductive, since a Meissner effect was observed.[32] This means that most clusters of D(−1) float in the magnetic field, above the actual magnet surface. Some types of small clusters like D_4 have no magnetic dipole[15] and will not float in the field, as observed in the experiments.[32] For this reason, it is interesting to investigate how a permanent magnetic field influences the fusion process.[4] The photons emitted may be an almost ideal probe of the processes at the magnet since they do not interact with the magnetic field. In Fig. 7, an experiment similar to that in Fig. 4 is shown, thus with variation of the laser pulse-frequency. The main differences between the results is that the peak with high-energy photons is lower on the magnet. This is an important difference but not always observed in similar experiments. Further, no thermal electrons from the plasma reach the collector. This is easily understood due to deflection of these electrons with relatively low energy in the field outside the magnet. The first negative spike which is due to electrons ejected from the chamber walls is the same in Figs. 4 and 7, showing that these electrons are formed far from the target (not influenced by the magnetic field) and probably also have high energy.

In Fig. 8, the ionizing photons with the laser probing the D(−1) layer on the magnet are observed as a function of the laser pulse-energy, at 532 nm laser-light. This figure may be compared with Fig. 5. The signal observed from the magnet is smaller, and also the thermal electron signal from the plasma is smaller. The most dramatic difference is however seen in the variation of the total charge with laser pulse-energy in panel (b), which has a typical high threshold on the magnet. The

(a)
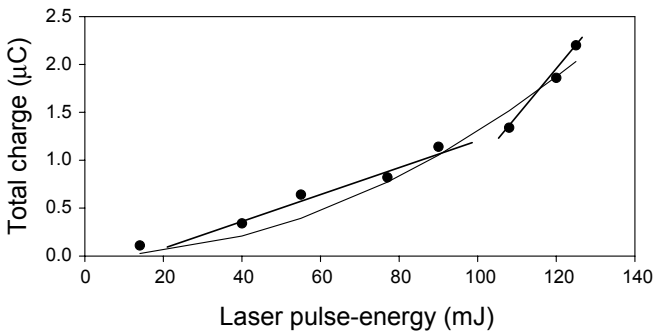
(b)

Fig. 6. Variation of the collector signal at 95 cm distance with laser pulse-energy in panel (a). The target was an Ir sample. The collector covered a fraction 4.4×10^{-4} of the full sphere. The charge in each curve is converted to the total charge per laser pulse assuming isotropic light emission in panel (b).

slope above threshold in Fig. 8(b) is however comparable to that in Fig. 5(b). At a slightly weaker magnetic field in Fig. 9 close to the magnet on the target, the signal is higher and comparable to Fig. 5, but the variation of total charge with laser pulse-energy still shows a threshold not observed in Figs. 5 and 6. Thus, it is concluded that a constant magnetic field of the strength used is not beneficial for the laser fusion process. This is as expected due to the Meissner effect, but still of interest to investigate.
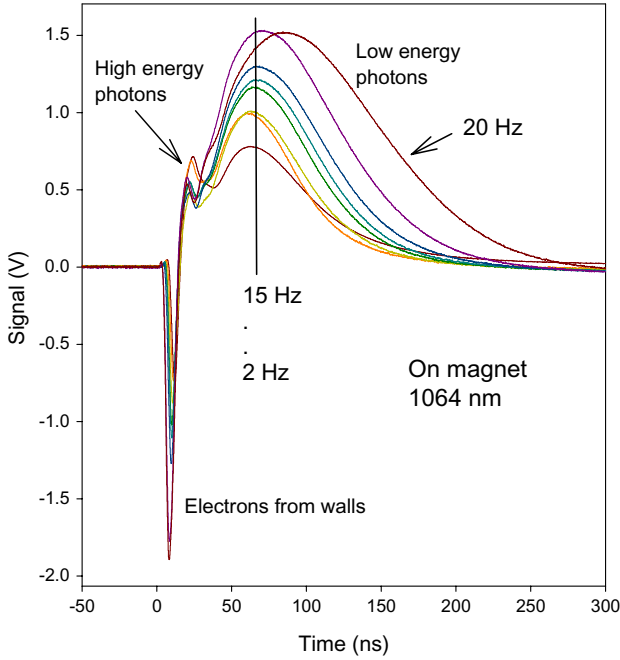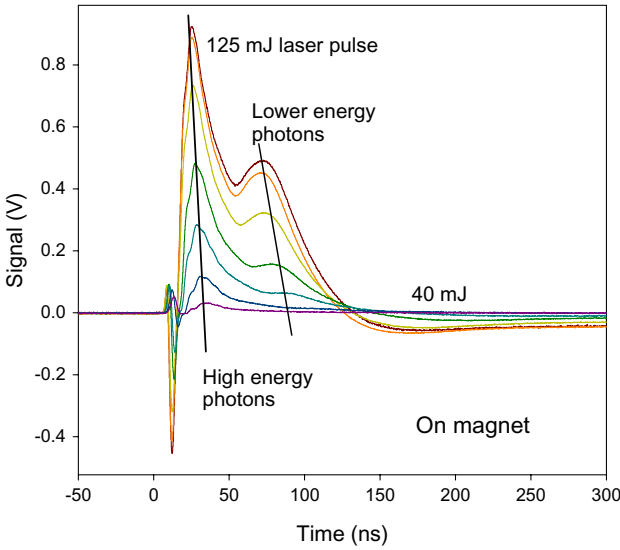
Fig. 7. Variation of the collector signal at 44 cm distance with laser pulse-frequency. Magnet surface sampled, 0.3 mbar D_2 pressure, 1064 nm light. Zero bias. Laser pulse-energy at 10 Hz was approximately 100 mJ.

(a)

Fig. 8. Variation of the collector signal at 44 cm distance with laser pulse-energy in panel (a). The laser focus was on the small permanent magnet. The collector covered a fraction 2.1×10^{-3} of the full sphere. The positive charge in each curve is converted to the total charge per laser pulse assuming isotropic light emission in panel (b).
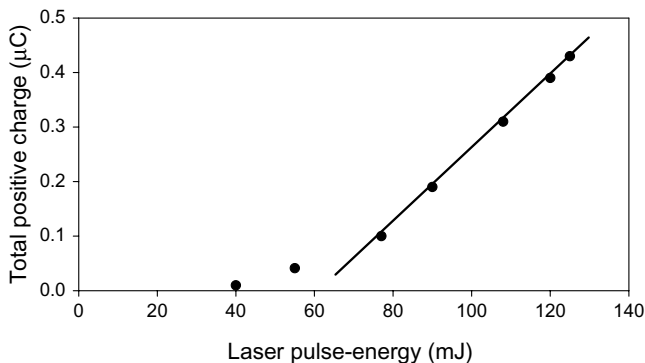
(b)

Fig. 8.   (*Continued*)

The laser photons at 532 nm have an energy of 2.33 eV, and at 1064 nm their energy is 1.17 eV. The measured signals are of similar size and shape in both cases. These photon energies are too low to give any photoelectrons at the collectors or the walls, which have a normal metal work function around 4 eV. Thus, photoemission due to scattered laser photons is highly unlikely, also since the signals are similar at the two wavelengths used. In Fig. 3, the signal at the collector at 61 cm (behind the cone collector) has the same shape as without the cone. This means that the signal is due to penetrating photons and not to visible photons at all. Photoelectrons from laser photons will have very low kinetic energy. Scattered laser photons can only exist during a very short time after the pulse impact, and will reach the collectors within 2–3 ns. The fast signal at such short times is dominated by high-energy photoelectrons or Compton electrons from the walls, definitely formed by ionizing photons with energy much larger than the work function of the surfaces. Thus, the contribution to the signal from scattered laser photons is negligible.

5. Discussion

To reach faster fusion processes and volume ignition in laser-induced fusion, it is necessary that the process efficiency varies faster-than-linear with the laser pulse-energy. Otherwise, the energy output is just linear with pulse-energy, and the energy gain does not increase with laser pulse-energy. Thus, the behavior observed for an Ir sample on the target in Fig. 6 is of great interest. It is possible that this behavior is not limited to catalytically active metals like Ir, but works also for other types of metals as carriers of D(−1). Recent results[4] may indicate that. A comparison between Figs. 5 and 6 shows that the fall-off for the total charge at high pulse-energy in Fig. 5 may to some extent be due to the thermal electron current from the plasma. This current makes it difficult to calculate the total positive charge accurately. This is supported by the data in Fig. 9, which give a linear behavior in the same range as the fall-off in Fig. 5. Thus, the fall-off may not be a typical
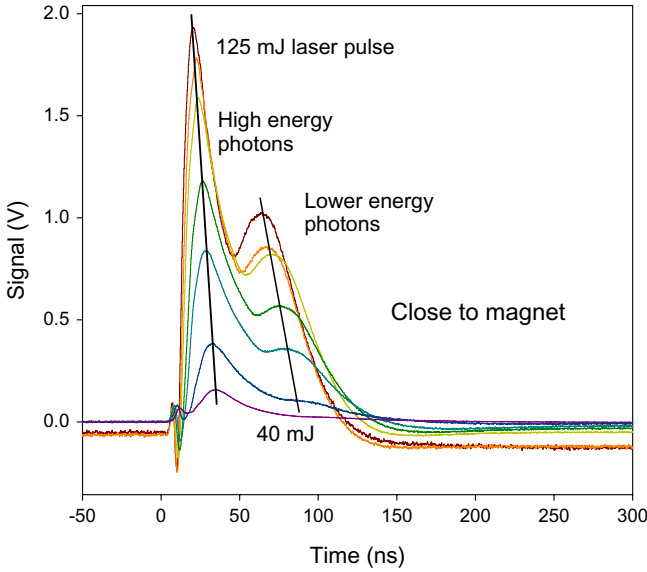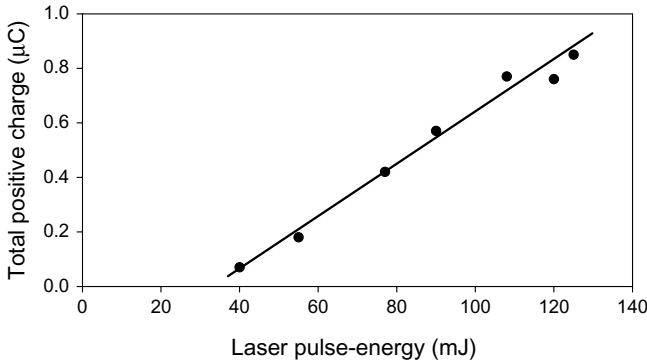
Fig. 9. Variation of the collector signal at 44 cm distance with laser pulse-energy in panel (a) with the laser focus close to the magnet on the stainless steel target plate. The collector covered a fraction 2.1×10^{-3} of the full sphere. The positive charge in each curve is converted to the total charge per laser pulse assuming isotropic light emission in panel (b).

result but the linear behavior is. The fast nonlinear increase in Fig. 6 is certainly important and may lead to volume ignition in fusion in $D(-1)$. However, due to the high cost of Ir, this is not the most suitable method for fusion in $D(-1)$. It may be thought that the normal linear behavior is due to a very thin layer of $D(-1)$ on a metal as the material where fusion is initiated. The important factor with Ir may be that $D(-1)$ not only forms a very thin layer, but also gives interstitial $D(-1)$ in the Ir surface layer. Such an effect is likely to give the rapidly increasing rate of fusion observed in Fig. 6(b).

Table 1.   Ranges for some fusion products. The databases at NIST (Ref. 37) are used for the proton ranges. For the neutrons, the quantity $(\sigma n)^{-1}$ is used as an approximate range with σ from ENDF (Ref. 38).

	Energy (MeV)	Range in D(−1) (nm)
p	3.02	0.66
	14.7	12
n	2.45	50
	14.1	150

The influence of a magnetic field on the fusion process was also studied. It was shown in Figs. 8 and 9 that a magnetic field gives a threshold type behavior, where the signal at low laser pulse-energy is almost nonexistent. A sizeable total charge is created only by relatively strong laser-pulses. This indicates that the magnetic field influences the structure of D(−1) which is known from other studies. A Meissner effect was observed in D(−1),[32] which means that the large chain-clusters in D(−1) do not reside on the magnet surface, but float in the magnetic field above the surface. This distance is probably less than 1 mm at the magnetic field strength used here. One problem with the laser-initiated fusion in D(−1) may be that a supporting metal surface is required to interact with (reflect or transform) the laser photons. With a distance from the surface which is much larger than the laser wavelength, the interaction with laser light may become too small. Another possibility is that the density of D(−1) is diminished by diffusion of the floating clusters away from the open magnet surface and down to the surface surrounding the magnet. The present results are not conclusive on this point, but it is clear that the magnetic field is not beneficial for the fusion process. However, the threshold behavior indicates a large difference in the processes, not only a difference in density of D(−1) on the magnet surface.

The results found here have implications for the design of useful fusion processes with ultra-dense deuterium D(−1), for example concerning the effects of a magnetic field. However, they are not so useful for the understanding of the fusion process taking place. In a previous publication,[3] it is shown that the range of neutrons with the typical energies given by normal D+D fusion in the D(−1) material is short. A neutron even with 14 MeV energy will only move approximately 150 nm in D(−1) of nominal density as shown in Table 1. Several other explanations of the apparent low neutron signal from the fusion processes in D(−1) (which will be published elsewhere) have been found by recent experimental work.

6. Conclusion

It is concluded that the energetic ionizing and penetrating photon emission from laser-induced processes in ultra-dense deuterium D(−1) can be observed. Higher energy photons with energy > 80 keV are emitted up to 30 ns after the laser pulse,

and lower energy photons from the plasma are emitted up to 150 ns after the laser pulse. Using catalytic metals like iridium in the target, a faster-than-linear variation of the total charge generated is detected. This is promising for reaching volume ignition. A constant magnetic field gives a high laser pulse-energy threshold for the total charge generated which is not beneficial for the fusion process. This effect is expected from the observed Meissner effect of the superconductive $D(-1)$.

Acknowledgments

References

1. S. Badiei, P. U. Andersson and L. Holmlid, *Laser Part. Beams* **28** (2010) 313.
2. P. U. Andersson and L. Holmlid, *J. Fusion Energy* **31** (2012) 249.
3. L. Holmlid, *Eur. Phys. J. A* **48** (2012) 11.
4. L. Holmlid, *Nucl. Instrum. Methods B* **296** (2013) 66.
5. L. Holmlid, *Laser Part. Beams* **31** (2013) 715.
6. S. Badiei, P. U. Andersson and L. Holmlid, *Int. J. Hydrog. Energy* **34** (2009) 487.
7. S. Badiei, P. U. Andersson and L. Holmlid, *Int. J. Mass Spectrom.* **282** (2009) 70.
8. P. U. Andersson and L. Holmlid, *Phys. Lett. A* **373** (2009) 3067.
9. L. Holmlid, H. Hora, G. Miley and X. Yang, *Laser Part. Beams* **27** (2009) 529.
10. S. Badiei, P. U. Andersson and L. Holmlid, *Phys. Scr.* **81** (2010) 045601.
11. P. U. Andersson and L. Holmlid, *Phys. Lett. A* **374** (2010) 2856.
12. S. Badiei, P. U. Andersson and L. Holmlid, *Appl. Phys. Lett.* **96** (2010) 124103.
13. P. U. Andersson, B. Lönn and L. Holmlid, *Rev. Sci. Instrum.* **82** (2011) 013503.
14. P. U. Andersson and L. Holmlid, *Phys. Lett. A* **375** (2011) 1344.
15. L. Holmlid, *Int. J. Mass Spectrom.* **304** (2011) 51.
16. L. Holmlid, *J. Clust Sci.* **23** (2012) 95.
17. P. U. Andersson and L. Holmlid, *Int. J. Mass Spectrom.* **310** (2012) 32.
18. P. U. Andersson and L. Holmlid, *Phys. Scr.* **86** (2012) 045601.
19. J. Nuckolls, L. Wood, A. Thiessen and G. Zimmerman, *Nature* **239** (1972) 139.
20. F. Winterberg, *The Release of Thermonuclear Energy by Inertial Confinement* (World Scientific, Singapore, 2010).
21. F. Olofson, A. Ehn, J. Bood and L. Holmlid, *Europhysics Conference Abstracts*, ed. S. Ratynskaya, Vol. 36F (Curran Associates, 2013), pp. 472–475, ISBN: 9781622769810.
22. J. D. Lindl, P. Amendt, R. L. Berger, S. G. Glendinning, S. H. Glenzer, S. W. Haan, R. L. Kauffman, O. L. Landen and L. J. Suter, *Phys. Plasmas* **11** (2004) 339.
23. O. A. Hurricane, D. A. Callahan, D. T. Casey, P. M. Celliers, C. Cerjan, E. L. Dewald, T. R. Dittrich, T. Döppner, D. E. Hinkel, L. F. Berzak Hopkins, J. L. Kline, S. Le Pape, T. Ma, A. G. MacPhee, J. L. Milovich, A. Pak, H.-S. Park, P. K. Patel, B. A. Remington, J. D. Salmonson, P. T. Springer and R. Tommasini, *Nature* **506** (2014) 343, doi: 10.1038/nature13008.
24. L. Holmlid, *J. Fusion Energy* **33** (2014) 348, doi: 10.1007/s10894-014-9681-x.
25. M. Tabak, J. Hammer, M. N. Glinsky, W. L. Kruer, S. C. Wilks, J. Woodworth, E. M. Campbell, M. D. Perry and R. J. Mason, *Phys. Plasmas* **1** (1994) 1626.
26. R. Betti, A. A. Solodov, J. A. Delettrez and C. Zhou, *Phys. Plasmas* **13** (2006) 100703.

27. L. Holmlid, *Int. J. Mod. Phys. E* **22** (2013) 1350089.
28. T. Guénault, *Basic Superfluids* (Taylor and Francis, London, 2003).
29. F. Winterberg, *J. Fusion Energy* **29** (2010) 317.
30. F. Winterberg, *Phys. Lett. A* **374** (2010) 2766.
31. F. Olofson and L. Holmlid, *J. Appl. Phys.* **111** (2012) 123502.
32. P. U. Andersson, L. Holmlid and S. R. Fuelling, *J. Supercond. Novel Magn.* 25 (2012) 873.
33. L. Holmlid, *Int. J. Mass Spectrom.* **352** (2013) 1.
34. F. Olofson and L. Holmlid, *Nucl. Instrum. Methods B* **278** (2012) 34.
35. G. R. Meima and P. G. Menon, *Appl. Catal. A* **212** (2001) 239.
36. M. Muhler, R. Schlögl and G. Ertl, *J. Catal.* **138** (1992) 413.
37. National Institute of Standards and Technology NIST, Physics Laboratory, PSTAR program.
38. National Nuclear Data Center, ENDF database, Brookhaven National Laboratory.